RSC Advances

PAPER

View Article Online
View Journal | View Issue

Published on 17 April 2015. Downloaded by Washington University in St. Louis on 30/12/2015 05:45:11.

Cite this: *RSC Adv.*, 2015, **5**, 37078

Dissociative ionization and Coulomb explosion of ethyl bromide under a near-infrared intense femtosecond laser field

Chong Teng, Hua Wu, Jian Zhang, Yan Yang, Tianqing Jia, Shian Zhang* and Zhenrong Sun*

Received 7th February 2015
Accepted 17th April 2015

DOI: 10.1039/c5ra02383a

www.rsc.org/advances

The multi-photon dissociation and Coulomb explosion of ethyl bromide C_2H_5Br under near-infrared (800 nm) femtosecond laser field are experimentally investigated by a DC-sliced ion imaging technique. The sliced images of fragment ions $C_2H_5^+$, Br^+, CH_3^+, CH_2Br^+, H_2^+ and $C_2H_3Br^+$ are obtained, and their dissociative pathways are assigned by observing their corresponding kinetic energy release (KER) and angular distribution. It is shown that low-KER components of these fragment ions result from multi-photon dissociation of singly charged parent ion $C_2H_5Br^+$, while high-KER components come from Coulomb explosion of doubly charged parent ion $C_2H_5Br^{2+}$. It is also shown that the precursor species $[C_2H_5^+...Br^+]$ has a longer lifetime than $[C_2H_3Br^+...H_2^+]$ and $[CH_3...CH_2Br^+]$. In addition, the probable H_2 and H_2^+ elimination channels are theoretically simulated by Gaussian 09 software packages, and the results show that the former is an asynchronous process while the latter is a synchronous process.

I. Introduction

When atoms or molecules are exposed to a femtosecond laser field with laser intensities in the range of 10^{13}–10^{15} W cm^{-2}, this intense femtosecond laser field will modify the potential energy surface (PES) of the electronic state in the atomic or molecular systems, and thus a variety of novel physical phenomena will occur, such as multi-photon ionization (MPI),[1–4] above threshold ionization (ATI),[5,6] high-order harmonic generation (HHG),[7,8] Coulomb explosion (CE),[9–12] and so forth. On the basis of these related phenomena, one can obtain the atomic or molecular dynamical processes. Alkyl bromide C_2H_5Br was usually taken as study example in the field of molecular dynamics under the intense laser field, and its photodissociation behaviors have been regarded as the reference for understanding photodissociation dynamics of polyatomic molecules.[13–15] In the photodissociation process of alkyl bromide, the dominant dissociation channel is C–Br bond fission to form an alkyl cation and a ground or spin–orbit excited state bromine atom,[16–20] and such observation has an important significance on the photochemical study of atmospheric bromine. Zhang *et al.* have experimentally studied the photodissociation dynamics of C–Br bond fission in a series of alkyl bromide by ultraviolet (UV) laser excitation,[13,21–23] and shown that fragments Br* ($^2P_{1/2}$) and Br ($^2P_{3/2}$) can be attributed to the perpendicular transition to the $^1Q_1$ and $^3Q_1$ states and the parallel transition to the $^3Q_0$ state. In addition to C–Br bond cleavage, Xu *et al.* have demonstrated other photodissociation pathways of ethyl bromide cation $C_2H_5Br^+$ based on 355 nm laser excitation,[24] and concluded that both $C_2H_5Br^+ \rightarrow C_2H_3^+ + H_2 + Br$ and $C_2H_5Br^+ \rightarrow C_2H_5^+ + HBr$ channels are produced through multi-center intermediates according to the anisotropy parameter. Gardiner *et al.* also confirmed above two dissociation channels by 266 and 355 nm laser excitations,[25] and theoretically simulated the lowest thermochemical threshold of accessible photofragmentation pathways from ethyl bromide cation $C_2H_5Br^+$, involving C–C, C–Br and C–H bond fissions.

In these previous studies, fragmentation dynamics of ethyl bromide by C–Br, C–C or C–H bond cleavage were usually performed by UV laser excitation, while studying them by near-infrared (IR) laser field was seldom reported. In this work, we present an investigation on the photodissociation process of ethyl bromide C_2H_5Br by 800 nm intense femtosecond laser field based on a DC sliced ion imaging technique. These fragment ions H_2^+, CH_3^+, $C_2H_5^+$, Br^+, CH_2Br^+ and $C_2H_3Br^+$ by C–C, C–Br and C–H bond fissions are observed, and low-KER components of these fragment ions are attributed to multi-photon dissociation (MPD) of singly charged parent ion $C_2H_5Br^+$ while high-KER components are assigned to Coulomb explosion (CE) of doubly charged parent ion $C_2H_5Br^{2+}$. Furthermore, elimination channels of H_2 and H_2^+ in MPD and CE processes are also experimentally observed, and the theoretical simulations show that the former is an asynchronous concerned process while the latter is a synchronous concerned process.

State Key Laboratory of Precision Spectroscopy, Department of Physics, East China Normal University, Shanghai 200062, People's Republic of China. E-mail: sazhang@phy.ecnu.edu.cn; zrsun@phy.ecnu.edu.cn

This journal is © The Royal Society of Chemistry 2015

Published on 17 April 2015. Downloaded by Washington University in St. Louis on 30/12/2015 05:45:11.

II. Experimental arrangement

Our experimental setup of DC sliced ion imaging system has been described in our earlier publications,[26,27] and here the simple statement is given. The multi-stage ion lens installed in the main chamber has the similar geometry designed by Suits *et al.*[28] According to ion trajectory simulation by Simon 8.0 software, the voltages applied on these electrodes are set to be $U_{\text{Repeller}} = 2000$ V, $U_1 = 1768$ V, $U_2 = 1661$ V and $U_3 = 0$ V, respectively. The ethyl bromide vapor seeded in helium gas at a backing pressure of 0.3 atm is expanded into the source chamber through a pulsed valve with a repetition rate of 100 Hz, and the supersonic molecular beam is skimmed before entering the reaction chamber. The femtosecond laser outputted from a regenerative amplification laser system has the center wavelength of 800 nm, pulse width of about 72 fs and repetition rate of 1 kHz, and the linearly polarized femtosecond laser pulse is focused into the reaction area by a lens with the focal length of 400 mm. The ethyl bromide is ionized and dissociated by the femtosecond laser field in the reaction chamber. These fragment ions are accelerated by multi-stage ion lens velocity apparatus and detected by a pair of 77 mm micro-channel plates (MCP) coupled to a P47 phosphor screen, and finally the sliced images of the fragment ions are recorded by an intensified charge-coupled device (ICCD) camera. To identify the fragment ion species, the time-of-flight (TOF) mass spectra are measured by a photomultiplier tube connected to a digital oscilloscope. In this experiment, all the timing sequence is controlled by Stanford Instrument Digital Delay/Pulse Generation (DG535).

III. Results and discussion

Fig. 1 shows three typical TOF mass spectra of ethyl bromide C_2H_5Br with the laser intensities of 1.8×10^{13} (a), 4.9×10^{13} (b) and 1.5×10^{14} W cm^{-2} (c), here the laser polarization direction is kept to be perpendicular to TOF axis. Since there are two different isotopes of bromine (^{79}Br and ^{81}Br) in nature, those fragment ions that contain bromine atom will exhibit multiple peak structure. The fragment ions $C_2H_m^+$ ($m = 2$–5) and singly charged parent ion $C_2H_5Br^+$ are observed with the laser intensity of 1.8×10^{13} W cm^{-2} (see Fig. 1(a)), which means that C–Br bond fission is the dominant dissociative channel in the lower laser intensities. When the laser intensity is increased to 4.9×10^{13} W cm^{-2}, these fragment ions H^+, H_2^+, CH_n^+ ($n = 0$–3) and Br^+ are observed (see Fig. 1(b)), and this illustrates the participation of C–C and C–H bond fissions. Here, the fragment ion H_3^+ is not observed, which may be due to the more complicated formation process comparing with the fragment ion H_2^+, which includes the breakage of three C–H bonds and formation of three H–H bonds, and therefore its formation need more demanding experimental condition. When the laser intensity is further increased to 1.5×10^{14} W cm^{-2}, highly charged fragment ions C^{2+} and Br^{2+} are observed (see Fig. 1(c)), which shows that the CE process will occur in the higher laser intensities. In this CE process, the ionization probability can be greatly enhanced when the bond length of the molecular ions

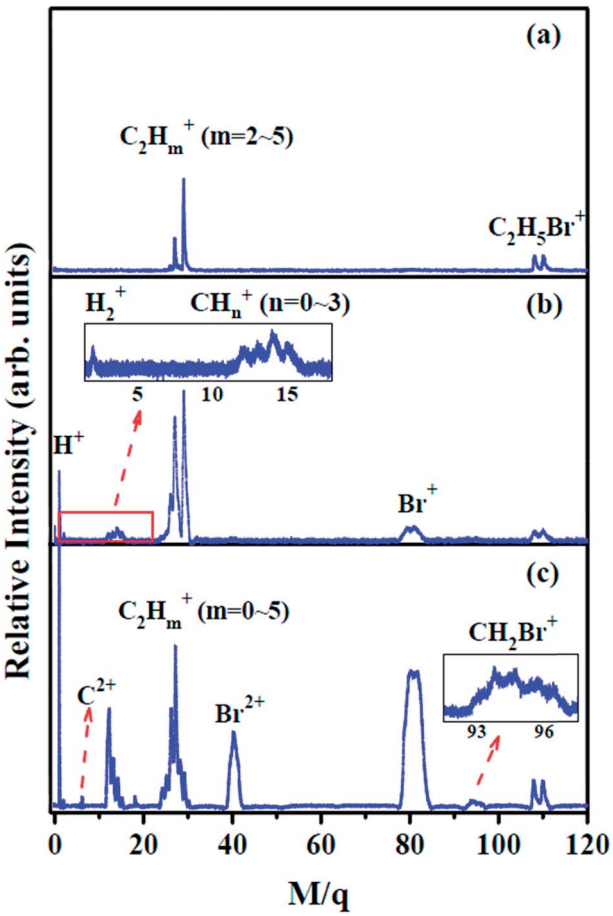

Fig. 1 TOF mass spectra of ethyl bromide C_2H_5Br under the femtosecond laser field with the laser intensities of 1.8×10^{13} (a), 4.9×10^{13} (b) and 1.5×10^{14} W cm^{-2} (c).

elongates to a critical distance, which triggers the Coulomb repulsion, and then the Coulomb repulsive energy accelerates the fragmentation process.[29,30] Therefore, the fragment ions produced by the Coulomb explosion process are easy to be observed in the higher laser intensities. In this work, our goal is to explore the photodissociation process *via* C–Br, C–C and C–H bond fissions.

DC sliced images can provide the related information of fragment ions, involving the KER and angular distributions. To further investigate the fragmentation dynamics of ethyl bromide under the intense femtosecond laser field, DC sliced images of fragment ions $C_2H_5^+$, Br^+, CH_3^+, CH_2Br^+, H_2^+ and $C_2H_3Br^+$ *via* C–Br, C–C and C–H bond fissions are obtained with the laser intensity of 1.1×10^{14} W cm^{-2}, and their corresponding velocity distributions are calculated, as shown in Fig. 2. Here, all velocity distributions are fitted with Gaussian function, and the peak velocities and kinetic energy releases are also labeled. It is noted that the fragment ion $C_2H_3Br^+$ cannot be observed in the mass spectrum because of its weak signal intensity, but it can be identified by our dc-sliced ion imaging system with high detection efficiency and sensitivity. In general, the fragment ions with low KER come from the MPD process of parent ions, while those with high KER come from the CE

Published on 17 April 2015. Downloaded by Washington University in St. Louis on 30/12/2015 05:45:11.

process.[26,31] Thus, these fragment ions with low KER in Fig. 2 should result from the MPD process of singly parent ion $C_2H_5Br^+$, and these corresponding MPD channels can be assigned as follows

C–Br bond cleavage:

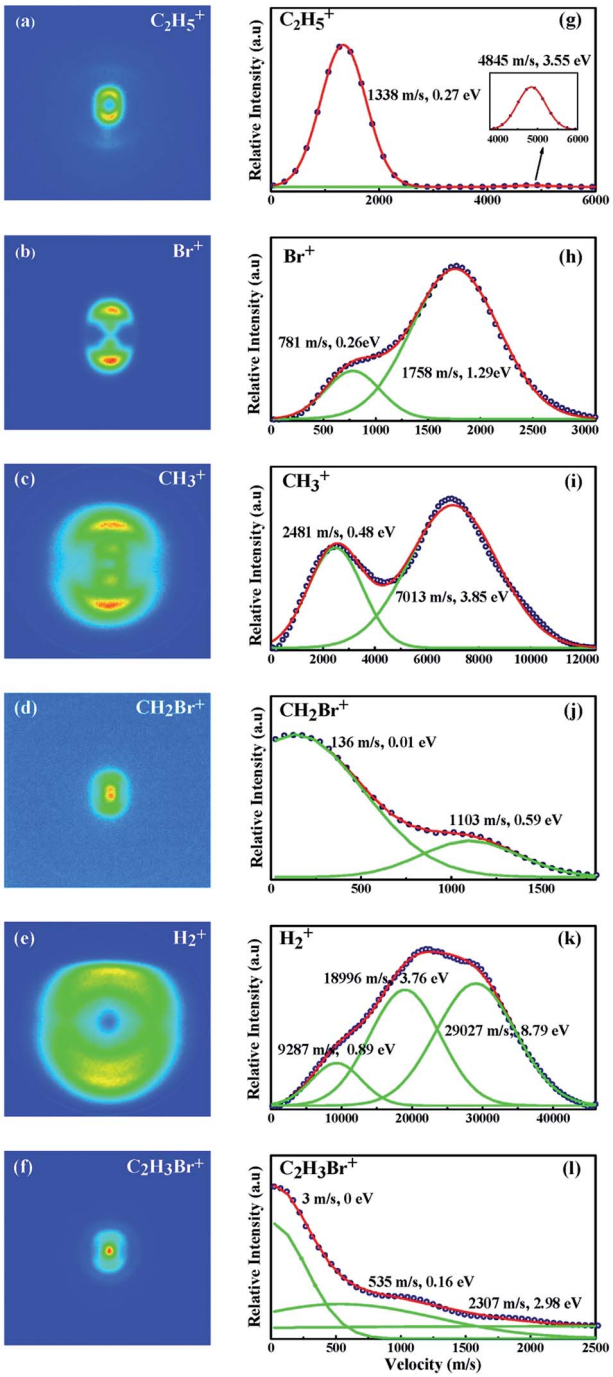

Fig. 2 DC sliced images of fragment ions $C_2H_5^+$ (a), Br^+ (b), CH_3^+ (c), CH_2Br^+ (d), H_2^+ (e) and $C_2H_3Br^+$ (f) with the laser intensity of 1.1×10^{14} W cm^{-2}, together with their corresponding KER distributions ((g)–(l)). The open circles (○) denote the experiment data, the solid lines (—) are the fitting Gaussian peaks, and the solid lines (—) are the simulated results.

$$C_2H_5Br \rightarrow Br + C_2H_5^+ + e^- \quad (1)$$

$$C_2H_5Br \rightarrow Br^+ + C_2H_5 + e^- \quad (2)$$

C–C bond cleavage:

$$C_2H_5Br \rightarrow CH_3 + CH_2Br^+ + e^- \quad (3)$$

$$C_2H_5Br \rightarrow CH_3^+ + CH_2Br + e^- \quad (4)$$

C–H bond cleavage:

$$C_2H_5Br \rightarrow H_2 + C_2H_3Br^+ + e^- \quad (5)$$

$$C_2H_5Br \rightarrow H_2^+ + C_2H_3Br + e^- \quad (6)$$

Under the intense femtosecond laser field, the ethyl bromide can also be ionized to the multi-charged parent ions, and then dissociates into fragment ions with high KER by Coulomb repulsive force. As well known, in the two-body CE model, the two fragment ions produced by the two-body CE process should have a relationship as follows[26,27,31,32]

$$\frac{KER(X^{p+})}{KER(Y^{q+})} = \frac{M(Y^{q+})}{M(X^{p+})} \quad (7)$$

where X and Y denote the two fragment ions, M is mass of fragment ions, and p and q are charge numbers of the ions. According to eqn (7), the two fragment ions Br^+ (1.29 eV) and $C_2H_5^+$ (3.55 eV) can be attributed to the CE channel as follows

$$C_2H_5Br \rightarrow Br^+ + C_2H_5^+ + 2e^- \quad (8)$$

Utilizing the same method, the two fragment ions CH_3^+ (3.85 eV) and CH_2Br^+ (0.59 eV) by C–C bond cleavage are also attributed to the following CE channel

$$C_2H_5Br \rightarrow CH_3^+ + CH_2Br^+ + 2e^- \quad (9)$$

Similarly, the two fragment ions H_2^+ (8.79 eV) and $C_2H_3Br^+$ (0.16 eV) by C–H bond cleavage can be assigned to such a CE channel

$$C_2H_5Br \rightarrow H_2^+ + C_2H_3Br^+ + 2e^- \quad (10)$$

To further investigate the CE process of doubly charged parent ion $C_2H_5Br^{2+}$, the angular distributions of these fragment ions from DC sliced images in Fig. 2 are extracted, and the calculated results are shown in Fig. 3. These experimental data are theoretically fitted by Legendre polynomial function,[33] and such a function is given as follows

$$I(\theta) = 1 + \sum_L a_L P_L(\cos^2\theta) \quad (L = 2, 4, 6) \quad (11)$$

where θ is the ejection angle of fragment ions measured from the laser polarization direction, which represents the instantaneous spatial distribution at the moment of CE process, a_L is the Legendre expansion coefficient, and the expectation value $\langle\cos^2\theta\rangle$ is the characterization of fragmentation anisotropy. The values of a_L and $\langle\cos^2\theta\rangle$ are summarized in Table 1. It is

This journal is © The Royal Society of Chemistry 2015

Published on 17 April 2015. Downloaded by Washington University in St. Louis on 30/12/2015 05:45:11.

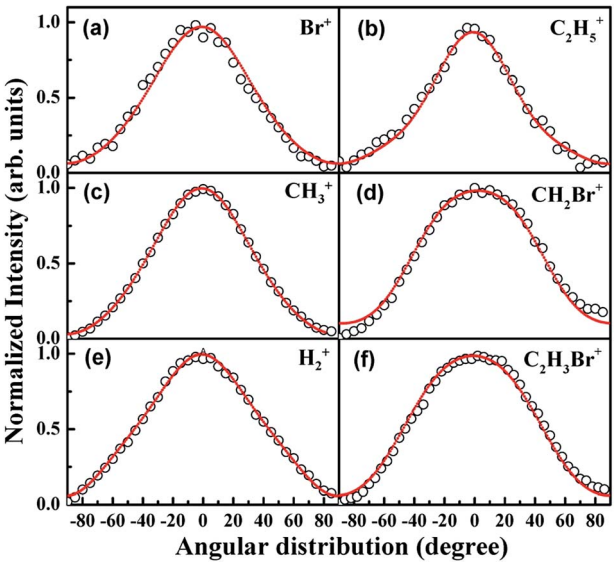

Fig. 3 Angular distributions of fragment ions $C_2H_5^+$ (a), Br^+ (b), CH_3^+ (c) and CH_2Br^+ (d). The open circles (o) are experimental data and the solid lines (—) are the simulated results by Legendre polynomial function.

Table 1 Legendre expansion coefficients a_L (L = 2, 4, 6) and expectation value $\langle\cos^2\theta\rangle$ of fragment ions $C_2H_5^+$, Br^+, CH_3^+, CH_2Br^+, H_2^+ and $C_2H_3Br^+$ by Coulomb explosion

Channels	Ions	a_2	a_4	a_6	$\langle\cos^2\theta\rangle$
(7)	$C_2H_5^+$	0.46	0.15	0.07	0.35
	Br^+	0.46	0.15	0.06	0.35
(8)	CH_3^+	0.59	0.10	0.03	0.41
	CH_2Br^+	0.61	0.04	−0.05	0.40
(9)	H_2^+	0.59	−0.01	0.05	0.39
	$C_2H_3Br^+$	0.61	0.04	−0.02	0.39

noted that the two fragment ions that come from the same CE channel show the similar expectation value $\langle\cos^2\theta\rangle$ (*i.e.*, fragmentation anisotropy), which can further confirm above photodissociation channel assignments in the CE process.

As known to all, when the short-lived precursor specie rotates as a whole in the space, its corresponding fragment ions will have stronger angular anisotropy. In Table 1, the leading expansion coefficient a_2 is an important anisotropy parameter, which characterizes the lifetime of the precursor specie state, and the precursor specie with the longer lifetime will induce the smaller a_2 value of the fragment ions.[33–35] In our experiment, the a_2 value by C–Br bond fission is determined to be $a_2 = 0.46$, which is smaller than that by C–C bond fission ($a_2 = 0.61$) as well as C–H bond fission ($a_2 = 0.61$). That is to say, the precursor specie $[C_2H_5^+\ldots Br^+]$ has the longer lifetime than $[C_2H_3Br^+\ldots H_2^+]$ and $[CH_3\ldots CH_2Br^+]$. This means that the precursor specie $[C_2H_5^+\ldots Br^+]$ is prepared in a deeper well of potential energy surface, and dissociates into the fragment ions $C_2H_5^+$ and Br^+ by Coulomb repulsive force following by the C–Br bond stretch.

As shown in eqn (5), (6) and (10), the elimination of H_2 or H_2^+ is the most complicated dissociative process that includes two C–H bond fissions and H–H bond formation. To understand how the fragment H_2 or H_2^+ is produced from the parent ion $C_2H_5Br^+$ or $C_2H_5Br^{2+}$, the probable photodissociation pathways are theoretically simulated by Gaussian 09 software packages.[36] The geometry of parent ions, transition states (TS) and dissociative products are optimized at the MP2 level with a 6-311++G(d,p) basis set. Meanwhile, the energies of related fragment ions are further refined by CCSD/6-311++G (d,p) with MP2 level zero-point energy corrections (ZPE). Fig. 4 shows the structure evolution during the formation of H_2 from the singly charged parent ion $C_2H_5Br^+$. The dissociation pathways of H_2 elimination from the same C atom and two C atoms are both calculated at the same theoretical level, and it is found that the energy barrier of H_2 elimination from two C atoms is much higher than from the same C atom, and so here only the H_2 elimination from the same C atom is presented. As shown in Fig. 4, the optimized geometry of parent ion $C_2H_5Br^+$ is with C–H bond lengths of 1.10 Å, ∠H–C–H of 109° and H–H distance of 1.78 Å. The elimination of H_2 starts with the C–H bond stretch to form TS. In the TS structure, two C–H bond lengths are elongated asymmetrically to 1.78 Å and 1.55 Å, ∠H–C–H is quickly decreased to 26°, and the distance between two H atoms is reduced to 0.79 Å, which is much shorter than that of parent ion $C_2H_5Br^+$. After surpassing TS with energy of 2.30 eV, the singly charged parent ion $C_2H_5Br^+$ dissociates into two parts $C_2H_3Br^+$ and H_2. The values of the three main parameters ∠H–C–H, two C–H bond lengths and H–H distance along reaction coordinates are listed in Table 2. As can be seen, ∠H–C–H is decreased, H–H distance is shortened, and the two C–H bond lengths are asymmetrically elongated due to the uneven distribution of surface charges in the two H atoms, which indicate that the $C_2H_5Br \rightarrow H_2 + C_2H_3Br^+$ elimination channel is an asynchronous concerned dissociation.

The energy path of H_2^+ elimination channel from doubly charged parent ion $C_2H_5Br^{2+}$ is shown in Fig. 5. It is noted that

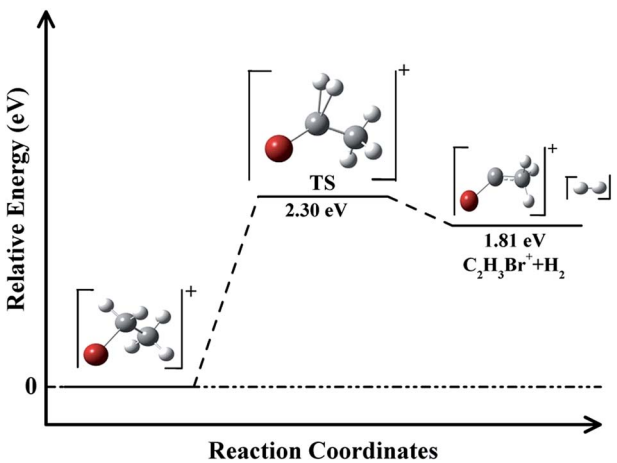

Fig. 4 The dissociation pathway for H_2 elimination from the singly charged parent ion $C_2H_5Br^+$, and here the theoretical simulation is performed at MP2/6-311++G (d,p) level.

Published on 17 April 2015. Downloaded by Washington University in St. Louis on 30/12/2015 05:45:11.

Table 2 Molecular structure evolution from the singly charged parent ion $C_2H_5Br^+$ characterized by the three main parameters ∠(H–C–H), two C–H bond lengths and H–H distance along the reaction coordinates calculated at MP2/6-311++G(d,p) level

∠H–C–H (°)	C–H bond lengths (Å)	H–H distance (Å)
109	1.10, 1.10	1.78
77	1.12, 1.16	1.42
46	1.20, 1.32	0.99
36	1.30, 1.48	0.88
26	1.55, 1.78	0.79
25	1.60, 1.83	0.78
21	1.91, 2.12	0.75
16	2.46, 2.61	0.74

Table 3 Molecular structure evolution from the doubly charged parent ion $C_2H_5Br^{2+}$ characterized by the three main parameters ∠(H–C–H), two C–H bond lengths and H–H distance) along the reaction coordinates calculated at MP2/6-311++G(d,p) level

∠H–C–H (°)	C–H bond lengths (Å)	H–H distance (Å)
37	1.37, 1.37	0.87
36	1.40, 1.40	0.86
33	1.48, 1.48	0.84
31	1.52, 1.52	0.83
26	1.61, 1.61	0.81
25	1.80, 1.80	0.78
21	2.07, 2.07	0.76
17	2.50, 2.50	0.75

the optimized geometry of $C_2H_5Br^{2+}$ is quite different from the structure of $C_2H_5Br^+$. The two C–H bonds are stretched to 1.37 Å, which are increased by 0.27 Å comparing with $C_2H_5Br^+$. Meanwhile, the distance between two H atoms is much closer, only 0.87 Å, which is almost half of the stable structure of $C_2H_5Br^+$. Such an observation indicates that Coulomb repulsive force will greatly change the molecular structure when the two electrons are stripped off under the intense femtosecond laser field. The elimination of H_2^+ also starts with the C–H bond stretch. In the TS structure, ∠H–C–H is decreased from 37° to 26°, the two C–H bond lengths are symmetrically elongated to 1.61 Å, and H–H distance is reduced to 0.81 Å. After surpassing TS, the doubly charged parent ion $C_2H_5Br^{2+}$ dissociates into the fragment ions H_2^+ and $C_2H_3Br^+$. It is noticeable that the energy of TS is lower (0.03 eV) than that of the doubly charged parent ion $C_2H_5Br^{2+}$, and this phenomenon has been demonstrated in previous studies.[37,38] That is to say, the doubly charged parent ion $C_2H_5Br^{2+}$ is trapped in a very shallow quasi-bound well of the potential energy surface, and can produce a barrierless reaction process. This conclusion can also be confirmed by the experimental observation that no doubly charged parent ion $C_2H_5Br^{2+}$ is observed in the full range of laser intensity. The values of the three main parameters ∠H–C–H, two C–H bond lengths and H–H distance are listed in Table 3. It is noted that the two C–H bonds are simultaneously broken and H–H bond is simultaneously formed, which shows that H_2^+ elimination from the doubly charged parent ion $C_2H_5Br^{2+}$ is a synchronous concerned process.

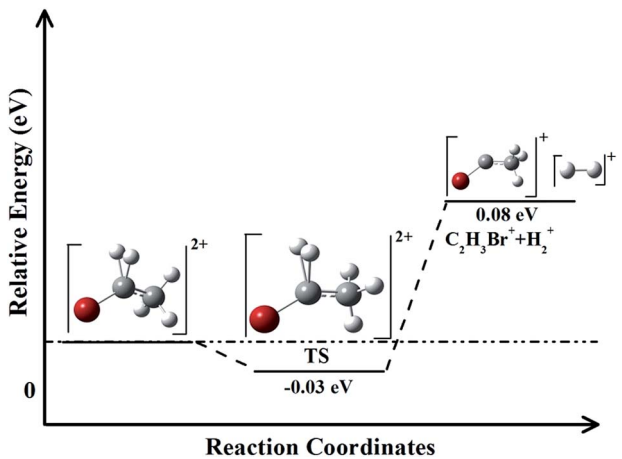

Fig. 5 The dissociation pathway for H_2^+ elimination from the doubly charged parent ion $C_2H_5Br^{2+}$, and here the calculation level is MP2/6-311++G (d,p).

IV. Conclusions

In summary, we have experimentally and theoretically studied the photodissociation process of ethyl bromide C_2H_5Br under the near-IR (800 nm) intense femtosecond laser field by the DC-slice imaging technique. These fragment ions $C_2H_5^+$, Br^+, CH_3^+, CH_2Br^+, H_2^+ and $C_2H_3Br^+$ by C–C, C–Br and C–H bond fissions were measured and their corresponding KER and angular distributions were calculated. We confirmed that these fragment ions with low KER are attributed to the MPD process of singly charged parent ion $C_2H_5Br^+$, while those components with high KER result from doubly charged parent ion $C_2H_5Br^{2+}$ *via* the CE process. The angular anisotropy of the fragment ions by the CE process suggested that the precursor specie $[C_2H_5^+ \ldots Br^+]$ has a longer lifetime than $[C_2H_3Br^+ \ldots H_2^+]$ and $[CH_3 \ldots CH_2Br^+]$. Moreover, the elimination channels of H_2 and H_2^+ were observed, and *ab initio* calculations showed that H_2 elimination is an asynchronous concerned reaction while H_2^+ elimination is a synchronous concerned reaction.

Acknowledgements

This work was partly supported by National Natural Science Fund (nos 51132004 and 11474096), and Shanghai Municipal Science and Technology Commission (no. 14JC1401500).

References

1 P. B. Corkum, Plasma Perspective on Strong-Field Multiphoton Ionization, *Phys. Rev. Lett.*, 1993, **71**, 1994.
2 J. E. Bayfield and P. M. Koch, Multiphoton Ionization of Highly Excited Hydrogen Atoms, *Phys. Rev. Lett.*, 1974, **33**, 258.

 This journal is © The Royal Society of Chemistry 2015

Published on 17 April 2015. Downloaded by Washington University in St. Louis on 30/12/2015 05:45:11.

3 A. J. Gotch and T. S. Zwier, Multiphoton Ionization Studies of Clusters of Immiscible Liquids. I. C_6H_6-$(H_2O)_n$, $n = 1, 2$, *J. Chem. Phys.*, 1992, **96**, 3388.
4 M. Castillejo, S. Couris, E. Koudoumas and M. Martín, Subpicosecond Ionization and Dissociation of Benzene and Cyclic Alkanes at 800 and 400 nm, *Chem. Phys. Lett.*, 1998, **289**, 303.
5 A. G. Suzor, X. He and O. Atabek, Above-Threshold Dissociation of H_2^+ in Intensity Laser Fields, *Phys. Rev. Lett.*, 1990, **64**, 515.
6 R. R. Freeman, P. H. Bucksbaum, H. Milchberg, S. Darack, D. Schumacher and M. E. Geusic, Above-Threshold Ionization with Subpicosecond Laser Pulses, *Phys. Rev. Lett.*, 1987, **59**, 1092.
7 J. J. Macklin, J. D. Kmetec and C. L. Gordon, High-Order Harmonic Generation Using Intense Femtosecond Pulses, *Phys. Rev. Lett.*, 1993, **70**, 766.
8 I. P. Christov, M. M. Murnane and H. C. Kapteyn, High-Harmonic Generation of Attosecond Pulses in the "Single-Cycle" Regime, *Phys. Rev. Lett.*, 1997, **78**, 1251.
9 X. G. Xue, C. Wu, Y. R. Liu, W. Huang, Y. K. Deng, Y. Q. Liu, Q. H. Gong and C. Y. Wu, Identifying Isomers of Carbon-dioxide Clusters by Laser-Driven Coulomb Explosion, *Phys. Rev. A: At., Mol., Opt. Phys.*, 2014, **90**, 033411.
10 K. Harumiya, H. Kono and Y. Fujimura, Intense Laser-field Ionization of H_2 Enhanced by Two-electron Dynamics, *Phys. Rev. A: At., Mol., Opt. Phys.*, 2002, **66**, 043403.
11 J. P. Nibarger, S. V. Menon and G. N. Gibson, Comprehensive Analysis of Srong-field Ionization and Dissociation of Diatomic Nitrogen, *Phys. Rev. A: At., Mol., Opt. Phys.*, 2001, **63**, 053406.
12 S. Das, P. M. Badani, P. Sharma, R. K. Vatsa, D. Das, A. Majumder and A. K. Das, Multiphoton Ionization and Coulomb Explosion of C_2H_5Br Cluster: A Mass Spectrometric and Charge Density Study, *Rapid Commun. Mass Spectrom.*, 2010, **25**, 1028.
13 B. F. Tang, R. S. Zhu, Y. Tang, L. Ji and B. Zhang, Photodissociation Dynamics of C_2H_5Br and n-C_3H_7Br in UV Region, *Chem. Phys.*, 2004, **303**, 37.
14 R. Montero, A. P. Conde, A. Longarte, F. Castaño, M. E. Corrales, R. de Nalda and L. Bañares, Femtosecond Time-resolved Photophysics and Photodissociation Dynamics of 1-Iodonaphthalene, *Phys. Chem. Chem. Phys.*, 2010, **12**, 7988.
15 A. Giuliani, F. M. Tollet, J. Delwiche, N. J. Mason, N. C. Jones, J. M. Gingell, I. C. Walker and M. J. H. Franskin, Electronic Excitation and Oscillator Strength of Ethyl Bromide by Vacuum Ultraviolet Photoabsorption and Electron Energy Loss Spectroscopy, *J. Chem. Phys.*, 2000, **112**, 6285.
16 B. Urban and V. E. Bongybey, One-color Multiphoton Threshold Photoelectron Spectra of Methyl Bromide, and Their Comparison with Methyl Iodide, *J. Chem. Phys.*, 2002, **116**, 4938.
17 A. G. Sage, T. A. A. Oliver, G. A. King, D. M. Murdock, J. N. Harvey and M. N. R. Ashfold, UV Photolysis of 4-iodo-, 4-bromo-, and 4-chlorophenol: Competitionbetween C–Y (Y = halogen) and O–H Bond Fission, *J. Chem. Phys.*, 2013, **138**, 164318.
18 T. Gougousi, P. C. Samartzis and T. N. Kitsopoulos, Photodissociation Study of CH_3Br in the First Continuum, *J. Chem. Phys.*, 1998, **108**, 5742.
19 S. Eden, P. L. Vieira, S. V. Hoffmann and N. J. Mason, VUV Photoabsorption in CF_3X (X = Cl, Br, I) Fluoro-Alkanes, *Chem. Phys.*, 2005, **323**, 313.
20 P. Zou, J. N. Shu, T. J. Sears, G. E. Hall and S. W. Northe, Photodissociation of Bromoform at 248 nm: Single and Multiphoton Processes, *J. Phys. Chem. A*, 2004, **108**, 1482.
21 C. H. Zhang, Z. Z. Cao, L. Q. Hua, Y. Chen and B. Zhang, Study on the Photodissociation Mechanisms of m-Bromotoluene at 234 and 267 nm Using Velocity Ion Imaging, *Chem. Phys. Lett.*, 2008, **454**, 171.
22 P. J. Liu, B. F. Tang and B. Zhang, Velocity Map Imaging of the Photolysis of n-C_4H_9Br in UV Region, *Chem. Phys.*, 2007, **340**, 141.
23 Y. M. Wang, S. Zhang, Q. S. Zheng and B. Zhang, C-Br bond fission dynamics in Ultraviolet Photodissociation of 1,2-dibromoethane, *Chem. Phys. Lett.*, 2006, **423**, 106.
24 D. D. Xu, R. J. Price, J. H. Huang and W. M. Jackson, Photodissociation of the Ethyl Bromide Cation at 355 nm by Means of TOF-MS and Ion Velocity Imaging Techniques, *Phys. Chem.*, 2001, **215**, 253.
25 S. H. Gardiner, T. N. V. Karsili, M. L. Lipciuc, E. Wilman, M. N. R. Ashfold and C. Vallance, Fragmentation Dynamics of the Ethyl Bromide and Ethyl Iodide Cations: A Velocity-Map Imaging Study, *Phys. Chem. Chem. Phys.*, 2014, **16**, 2167.
26 Y. Yang, L. L. Fan, S. Z. Sun, J. Zhang, Y. T. Chen, S. A. Zhang, T. Q. Jia and Z. R. Sun, Dissociation Double Ionization of 1-Bromo-2-Chloroethane Irradiated by an Intense Femtosecond Laser Field, *J. Chem. Phys.*, 2011, **135**, 064303.
27 H. Wu, Y. Yang, S. Z. Sun, J. Zhang, L. Deng, S. A. Zhang, T. Q. Jia, Z. G. Wang and Z. R. Sun, Concerted Elimination of Br_2^+ Resulting from the Coulomb Explosion of 1,2-Dibromoethane in an Intense Femtosecond Laser Field, *Chem. Phys. Lett.*, 2014, **607**, 70.
28 D. Townsend, M. P. Minitti and A. G. Suits, Direct Current Slice Imaging, *Rev. Sci. Instrum.*, 2003, **74**, 2530.
29 A. Giuliani, F. M. Tollet, J. Delwiche, N. J. Mason, N. C. Jones, J. M. Gingell, I. C. Walker and M. J. H. Franskin, Electronic Excitation and Oscillator Strength of Ethyl Bromide by Vacuum Ultraviolet Photoabsorption and Electron Energy Loss Spectroscopy, *J. Chem. Phys.*, 2000, **112**, 6285.
30 I. Bocharova, R. Karimi, E. F. Penka, J. P. Brichta, P. Lassonde, X. Q. Fu, J. C. Kieffer, A. D. Bandrauk, I. Litvinyuk, J. Sanderson and F. Légaré, Charge Resonance Enhanced Ionization of CO_2 Probed by Laser Coulomb Explosion Imaging, *Phys. Rev. Lett.*, 2011, **107**, 063201.
31 H. Wu, S. A. Zhang, Y. Yang, S. Z. Sun, J. Zhang, L. Deng, T. Q. Jia, Z. G. Wang and Z. R. Sun, Coulomb Explosion and Dissociative Ionization of 1,2-Dibromoethane under an Intense Femtosecond Laser Field, *RSC Adv.*, 2014, **4**, 45300.
32 J. Zhang, S. A. Zhang, Y. Yang, S. Z. Sun, H. Wu, J. Li, Y. T. Chen, T. Q. Jia, Z. G. Wang, F. A. Kong and Z. R. Sun,

Published on 17 April 2015. Downloaded by Washington University in St. Louis on 30/12/2015 05:45:11.

Photodissociation of Br_2 Molecules in an Intense Femtosecond Laser Feld, *Phys. Rev. A: At., Mol., Opt. Phys.*, 2014, **90**, 053428.

33 T. Okino, Y. Furukawa, P. Liu, T. Ichikawa, R. Itakura, K. Hoshina, K. Yamanouchi and H. Nakano, Coincidence Momentum Imaging of Ejection of Hydrogen Molecular Ions From Methanol in Intense Laser Fields, *Chem. Phys. Lett.*, 2006, **419**, 223.

34 S. Z. Sun, Y. Yang, J. Zhang, H. Wu, Y. T. Chen, S. A. Zhang, T. Q. Jia, Z. G. Wang and Z. R. Sun, Ejection of Triatomic Molecular Ion H_3^+ from Methyl Chloride in an Intense Femtosecond Laser Field, *Chem. Phys. Lett.*, 2013, **581**, 16.

35 Y. Furukawa, K. Hoshina, K. Yamanouchi and H. Nakano, Ejection of Triatomic Hydrogen Molecular Ion from Methanol in Intense Laser Fields, *Chem. Phys. Lett.*, 2005, **414**, 117.

36 M. J. Frisch, G. W. Trucks, H. B. Schlegel, G. E. Scuseria, M. A. Robb, J. R. Cheeseman, G. Scalmani, V. Barone, B. Mennucci, G. A. Petersson, *et al.*, *Gaussian 09, revision B.01*, Gaussian, Inc., Wallingford, CT, 2010.

37 Y. X. Zhao, X. N. Wu, J. B. Ma, S. G. He and X. L. Ding, Experimental and Theoretical Study of the Reactions between Vanadium-Silicon Heteronuclear Oxide Cluster Anions with *n*-Butane, *J. Phys. Chem. C*, 2010, **114**, 12271.

38 X. N. Wu, Y. X. Zhao, W. Xue, Z. C. Wang, S. G. He and X. L. Ding, Active Sites of Stoichiometric Cerium Oxide Cations $(Ce_mO_{2m}^+)$ Probed by Reactions with Carbon Monoxide and Small Hydrocarbon Molecules, *Phys. Chem. Chem. Phys.*, 2010, **12**, 3984.

This journal is © The Royal Society of Chemistry 2015